

# Development of tungsten fibre-reinforced tungsten composites towards their use in DEMO – Potassium doped tungsten wire

J Riesch<sup>1,\*</sup>, Y Han<sup>1</sup>, J Almanstötter<sup>3</sup>, J W Coenen<sup>2</sup>, T Höschen<sup>1</sup>, B Jasper<sup>2</sup>, P Zhao<sup>1</sup>,  
Ch Linsmeier<sup>2</sup> and R Neu<sup>1,4</sup>

<sup>1</sup> Max-Planck-Institut für Plasmaphysik, 85748 Garching, Germany

<sup>2</sup> Forschungszentrum Jülich GmbH, Institut für Energie und Klimaforschung – Plasmaphysik, 52425 Jülich,  
Germany

<sup>3</sup> OSRAM GmbH, Corporate Technology CT TSS MTS MET, 86830 Schwabmünchen, Germany

<sup>4</sup> Fakultät für Maschinenbau, Technische Universität München, D-85748 Garching, Germany

\*Corresponding author: johann.riesch@ipp.mpg.de

**Abstract.** For the next step fusion reactor the use of tungsten is inevitable to suppress erosion and allow operation at elevated temperature and high heat loads. Tungsten fibre-reinforced composites overcome the intrinsic brittleness of tungsten and its susceptibility to operation embrittlement and thus allow its use as a structural as well as an armour material. That this concept works in principle has been shown in recent years. In this contribution we present a development approach towards their use in a future fusion reactor. A multilayer approach is needed addressing all composite constituents and manufacturing steps. A huge potential lies in the optimization of the tungsten wire used as fibre. We discuss this aspect and present studies on potassium doped tungsten wire in detail. This wire, utilized in the illumination industry, could be a replacement of the so far used pure tungsten wire due to its superior high temperature properties. In tensile tests the wire showed high strength and ductility up to an annealing temperature of 2200 K. The results show that the use of doped tungsten wire could increase the allowed fabrication temperature and the overall working temperature of the composite itself.

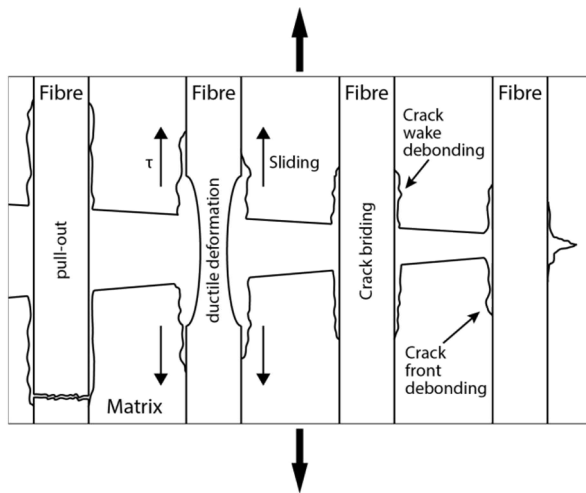
## 1. Introduction

29 Materials with advanced capabilities are essential for the successful design of the next step  
30 fusion reactor, i.a. DEMO, and are crucial for a fusion power plant. The use of tungsten is  
31 inevitable to suppress erosion and to allow operation at elevated temperature and high heat  
32 loads [1]. However tungsten suffers from an intrinsic brittleness below a certain temperature,  
33 the so called ductile-to-brittle transition temperature [2,3]. Depending on mechanical,  
34 chemical and (micro-)structural conditions this temperature is between 500 and 900 K. In  
35 addition W is susceptible to be further embrittled by overheating or neutron irradiation [4].

36 Tungsten fibre-reinforced tungsten composites ( $W_f/W$ ) utilize extrinsic toughening  
37 mechanisms like crack bridging by intact fibres or frictional pull-out of broken fibres. Similar  
38 to ceramic fibre-reinforced ceramics [5] the overall toughness is increased and the brittleness  
39 problem of W is mitigated. Hence an application as a plasma facing material under thermal  
40 transients and neutron bombardment now seems feasible.

41 That extrinsic toughening works in  $W_f/W$  has been shown at the Max-Planck-Institute for  
42 Plasma Physics, Garching (IPP) in the past years [6,7]. As a key factor for the feasibility of  
43 this toughening mechanism the interface between fibre and matrix was investigated in a first  
44 step [8,9]. The feasibility of the toughening effect itself was shown on model systems  
45 consisting of a single fibre embedded in the matrix material. With this method the major  
46 contribution of the plastic fibre deformation to the toughening was shown [10]. In addition it  
47 was proven that the toughening mechanisms are still active after a full change of the  
48 microstructure by recrystallization [11]. Figure 1 shows a summary of the active toughening  
49 effects in  $W_f/W$ . In a further development step a fabrication method based on the chemical  
50 deposition of W was developed and first bulk samples were produced [12]. Mechanical tests  
51 on these samples revealed an intense toughening. Based on these results the material was  
52 chosen as risk mitigation PFC/HHF (plasma facing component/high heat flux) material in the  
53 EU Fusion roadmap [13]. In summary the idea of extrinsic toughening in W works in  
54 principle and the application as highly loaded divertor element is identified. Thus level 2 of

55 the so called technology readiness level (TRL) is reached (proof-of-principle + application  
56 formulated) (explanation of TRL concept in [14]).



57

58 *Figure 1: Toughening mechanism in tungsten fibre-reinforced composites.*

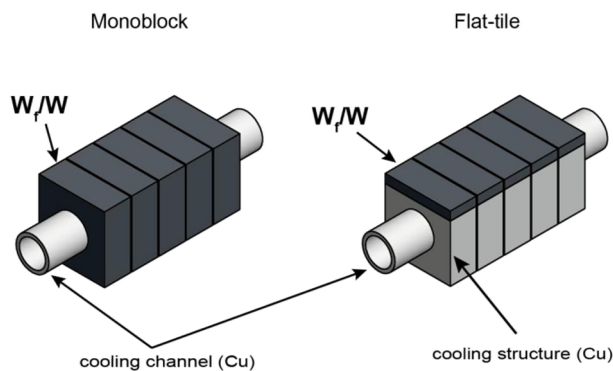
59

60 Candidate materials for DEMO however need to reach TRL 6-8 before being considered for  
61 design [15]. The first step in this development is to prove that the concept of a  $W_f/W$  divertor  
62 element works (TRL3, proof-of-concept) and to validate it under relevant testing conditions  
63 (TRL4, validation). TRL 5 is typically associated with the validation in a relevant  
64 environment. In the case of  $W_f/W$  this is associated with the plasma interaction, e.g. regarding  
65 hydrogen retention or erosion, and the behavior under neutron irradiation. TRL 6 will be  
66 reached by a prototype demonstration in a relevant environment. This can be in wall tiles of  
67 existing fusion reactors, e.g. on a manipulator or as a long term wall tile.

68 As a first step it has been chosen to fabricate  $W_f/W$  components and test them under cyclic  
69 high heat flux conditions. These components will be designed close to the ITER reference-  
70 design. In figure 2 two possible versions for such a mock-up are shown. The loading will be  
71 performed in the ion beam facility GLADIS in Garching, Germany [16,17] and/or the electron  
72 beam facility JUDITH 1 [18]. Cyclic extreme loading allows the evaluation of the maximum  
73 strength, the fatigue strength and the damage tolerance/toughness and thus provides the  
74 conceptual proof in one step. The concentration on one main test provides clear constraints

75 for geometry and test methodology. This leads to a distinct structure and allows a target-  
76 oriented approach. For the successful realization and evaluation of such experiments the  
77 complete characterization of the material is essential. In summary this allows not only to  
78 show that the concept works but also qualifies  $W_f/W$  for future applications, e.g. in a DEMO  
79 divertor (TRL 4).

80



81

82 *Figure 2: Monoblock and Flat tile mock-up for high heat flux tests*

83

84 For the component production and the following testing all constituents of the composite, i.a.  
85 fibre, interface and matrix, and all manufacturing steps, i.a. interface coating, fibre positioning  
86 and matrix production, will be addressed. Utilizing the so far used techniques, a pure tungsten  
87 fibre, an oxidic interface and a chemically deposited matrix as a starting point, new  
88 techniques will be investigated and/or established techniques will be optimized. As all these  
89 aspects are strongly linked, e.g. the manufacturing temperature of the W matrix with the high  
90 temperature stability of the W fibre or the interface, this is a multilayer approach.

91 As an example we discuss in this paper the role of the tungsten wire used as fibre and  
92 especially the influence of annealing on its mechanical properties. A screening test on  
93 potassium doped tungsten wire is presented in detail. As this is strongly related to the allowed  
94 matrix manufacturing temperatures, a short review is given on matrix production techniques  
95 at first.

96

## 97 **2. Fabrication of the tungsten matrix in $W_f/W$ composites**

98 The very high melting point and high temperature strength both for fibre and matrix do not  
99 allow for classical composite production routes (examples in [5]). It is furthermore important  
100 that the properties of fibre and interface are not degraded during the process. Chemical  
101 deposition techniques allow low processing temperatures ( $< 900$  K) and a force-less  
102 fabrication, and thus the preservation of the interface and fibre integrity as well as fibre  
103 topology. In this process tungsten hexafluoride is reduced by hydrogen in a heterogeneous  
104 surface reaction and thus solid tungsten is formed.

105 So far surface deposition processes (chemical vapour deposition – CVD) have been used for  
106 the production of model systems containing a single fibre [8] and infiltration techniques  
107 (chemical vapour infiltration – CVI) have been investigated to produce larger samples. The  
108 infiltration process can be influenced by varying the fibre arrangement, the gas flow and the  
109 temperature. In a dual step infiltration process Riesch et al. were able to produce first bulk  
110  $W_f/W$  for mechanical testing [12]. A key issue is the optimization of this tungsten matrix  
111 production process allowing the production of larger, reproducible samples. A chemical  
112 deposition device (WILMA) which has been specifically designed for the chemical deposition  
113 of tungsten for the matrix production in  $W_f/W$  was installed at the Forschungszentrum Jülich  
114 (FZJ).

115 Although CVD processes have the advantage of low production temperature and the absence  
116 of mechanical impact, powder metallurgical (PM) routes would allow several interesting  
117 benefits. The most important benefit is that the production and processing techniques are  
118 highly developed as PM is the standard process for tungsten bulk production. This would give  
119 potential for an easier optimisation and adoption of the matrix properties. For example it  
120 would be easier to implement alloying, e.g. self passivating tungsten. Nevertheless the

121 required high temperature and pressure might be a severe drawback regarding degradation of  
122 fibre or interface properties.

123 PM investigations on single fibre composites have been started in order to understand the  
124 interaction between fibre, interface and matrix. Hot isostatic pressing (HIP) was applied to  
125 produce a dense W matrix with and without embedded fibres. First samples at various HIPing  
126 temperature up to 2200 K have been produced and mechanical testing including fibre push out  
127 has been performed. These tests show that the interface properties are critical for the path  
128 forward within the HIPing approach. A detailed description of these tests and their results is  
129 given by Jasper et al. [19].

130 In these tests pure tungsten wire was used as fibres. These fibres were fully recrystallized  
131 during the HIP process. As recrystallized fibres possess very poor mechanical properties  
132 compared to as-fabricated ones [20] this is a severe drawback for PM production route. As a  
133 loophole potassium doped fibres are known for their high temperature stability and could be a  
134 solution. In the following we present experiments on the mechanical properties after high  
135 temperature annealing to investigate this option.

136

### 137 **3. Mechanical properties of W-wire used as fibre in $W_f/W$ composites**

138 A key benefit of  $W_f/W$  under cyclic high heat loads are the exceptional properties of the  
139 tungsten wires used as fibres: Pure as well as potassium doped tungsten wires show  
140 exceptional ductility and strength at room temperature in contrast to conventional bulk  
141 tungsten being brittle at room temperature. These are ideal properties facilitating the  
142 toughening in  $W_f/W$  as the high strength is important for the bridging effect and ductile  
143 deformation allows the dissipation of substantial amount of energy (compare mechanism in  
144 figure 1).

145 Pure tungsten wires have been investigated by Zhao et al. [20] by means of tensile tests.  
146 Wires in the as-fabricated state and after annealing for 3 h at 1273 K and 30 minutes at 1900

147 K were tested. The as-fabricated and the low heat treated fibres showed ductile behaviour and  
148 a strength of more than 2900 MPa and 1900 MPa respectively. In contrast to that the high  
149 temperature heat treated fibres failed in a brittle manner with a mean strength of  
150 approximately 900 MPa, and a high scatter. In the following we present similar experiments  
151 on potassium doped tungsten wire.

### 152 *3.1 Sample preparation*

153 Drawn tungsten wire doped with 60-75 ppm potassium was used for tensile tests. The wire  
154 was produced and provided by the OSRAM GmbH, Schwabmünchen. The measured diameter  
155 of the wire was  $148.7 \pm 0.2 \mu\text{m}$ . The wire was cut into pieces and straightened by tensile  
156 loading until fracture (displacement rate of  $100 \mu\text{m/s}$ ). The straightened wires were cut into  
157 80 mm long pieces to get rid of the damaged zone. The 80 mm wire pieces are called fibres in  
158 the following.

159 Fibres in the as-fabricated state and after annealing were tested. 5 different annealing  
160 temperatures are investigated (see table 1). The annealing was done in a tube furnace under  
161 hydrogen atmosphere. The holding time was 30 min in each case.

162 Temperature 1-3 are below the reported temperature of extensive grain growth in potassium  
163 doped wire (2100-2300 K [21]), temperature 4 is around this region and temperature 5 is well  
164 above it. In addition temperature 1 and 3 are similar to the annealing temperatures in pure  
165 tungsten wire studies [20] and therefore allow a direct comparison.

166 In figure 3 optical micrographs of longitudinal sections are shown for the different sample  
167 types. The extensive grain growth leading to very big grains is clearly visible for the sample  
168 annealed at 2573 K.

169

170 *Table 1: Annealing temperature*

---

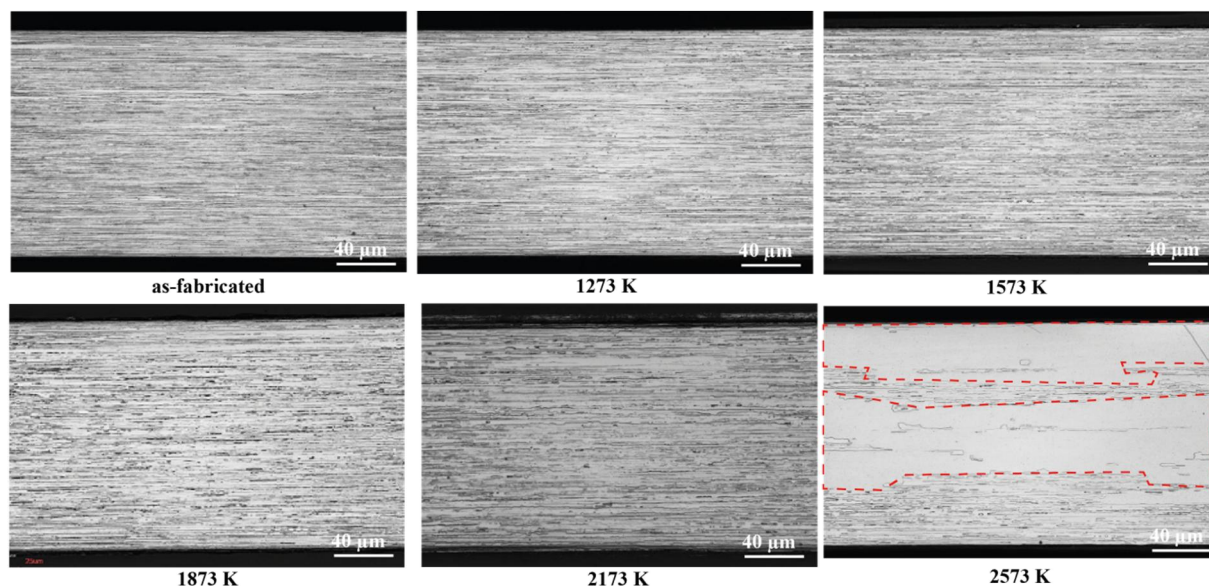
<i>T 0</i>	<i>T 1</i>	<i>T 2</i>	<i>T 3</i>	<i>T 4</i>	<i>T 5</i>
------------	------------	------------	------------	------------	------------

---

*Annealing*

<i>temperature</i>	-	1273	1573	1873	2173	2573
<i>[K]</i>						

171



172

173 *Figure 3 Longitudinal sections (optical) of potassium doped tungsten wire at different*  
 174 *annealing stages. The dashed lines in the 2573 K case indicate large grains after secondary*  
 175 *grain growth.*

176

177 *3.2 Experimental*

178 The tensile tests were performed with a universal testing machine (TIRA Test 2820) at room  
 179 temperature. The load is measured by a 200 N range load cell. The displacement was  
 180 measured contactless by a laser speckle extensometer (LSE-4000 DE) using the interference  
 181 pattern of two laser spots. This measurement requires a perfectly aligned sample. To align the  
 182 fibre within the tension axis a preload (between 10-15 N  $\cong$  550-850 MPa) is applied and the  
 183 lower sample holder is moved until a load minimum is reached. Still the displacement record  
 184 was not always reliable.



185 The measuring length is defined by the distance between the two laser spots and was  
186 approximately 18 mm for all tests. Only if the fibre fractures within this zone the test is  
187 assigned as valid. To ensure that the fibre fractures within the measuring length both ends of  
188 the fibre are attached to paper by gluing (UHU Plus endfest 300). Thus the cross-section in  
189 these parts is enlarged and the probability of fracture is decreased. The uncovered part was  
190 approximately 20 mm for all tests. The tests were conducted in a displacement controlled  
191 mode with a displacement rate of 5  $\mu\text{m/s}$ .

192

#### 193 **4. Results**

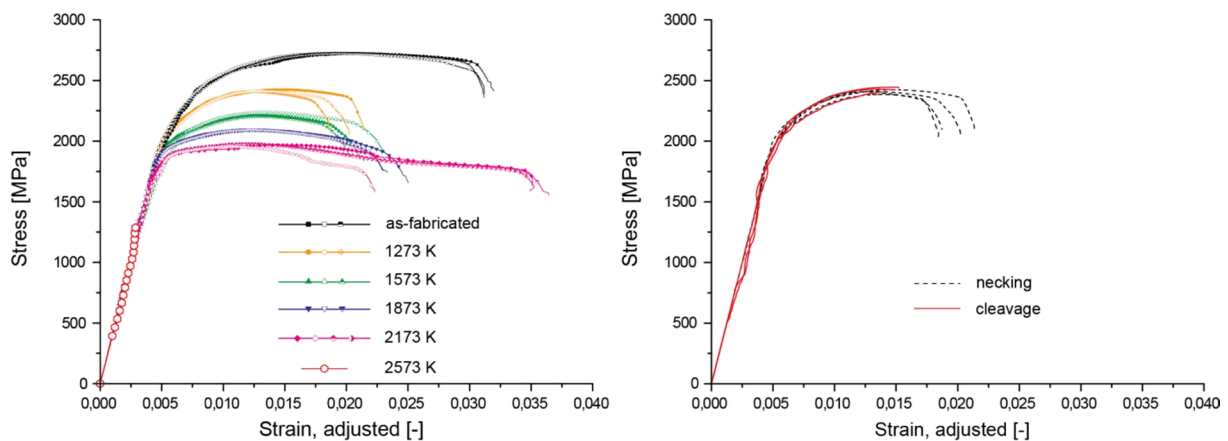
194 Figure 4 (left) shows typical stress-strain curves of the tested wires. The region of elastic  
195 response was extrapolated to the origin (dotted line). Due to unreliable strain measurements  
196 the estimated Young's moduli show significant deviation between 280 and 440 GPa. To be  
197 able to compare the different annealing stages the strain axis was corrected to meet 400 GPa  
198 in the elastic region. However as the variations are quite significant we do not give any  
199 quantitative values besides the ultimate strength which is independent of the displacement  
200 measurement. Nevertheless trends are obvious for other mechanical properties like yield  
201 strength and fracture strain.

202 In all cases an elastic deformation is observed for low strain. Except for the 2573 K case this  
203 is followed by an extended phase of plastic deformation. If plastic deformation occurs the  
204 stress decreases moderately after reaching the ultimate strength. This goes on until a faster  
205 drop occurs near final fracture. Samples annealed at 1273K do not show this drop in 8 out of  
206 24 cases and fail near to the maximum load. Typical curves for both cases are shown in  
207 Figure 4 (right). However yield strength and ultimate strength of these samples are  
208 comparable. The mean value for the ultimate strength of the different sample types is given in  
209 table 2. The errors are calculated by the standard deviation of the mean. For each temperature

210 6 valid measurements are considered. 16 samples have been taken into account for annealing  
 211 temperature of 2573 K to give a better statistic in the brittle case.

212 In the as-fabricated case work hardening of approximately 2 % is observed. The work  
 213 hardening becomes less with increased annealing temperature. For the samples annealed at  
 214 2173 K almost no work hardening is observed. The fracture strain drops with the first  
 215 annealing step and stays almost constant for the next higher temperatures. For the annealing  
 216 temperature of 2173 K it increases significantly and is even larger as in the as-fabricated case.  
 217 However one out of 6 tested samples shows a lower fracture strain at this annealing stage. The  
 218 yield strength as well as the ultimate strength decrease with rising annealing temperature.

219



220

221 *Figure 4: Typical stress-strain curves of tensile tests of potassium doped tungsten wire at*  
 222 *different annealing stages (left). Three samples are shown for the as-fabricated case and an*  
 223 *annealing temperature of 1273 K, 1573 K and 1873 K. A fourth sample having a much lower*  
 224 *fracture strain is shown for annealing temperatures 2173 K. For the sake of clarity only one*  
 225 *curve is shown for temperature 2573 K. For an annealing temperature of 1273 K fracture*  
 226 *with necking as well as cleavage dominated occurred (right).*

227

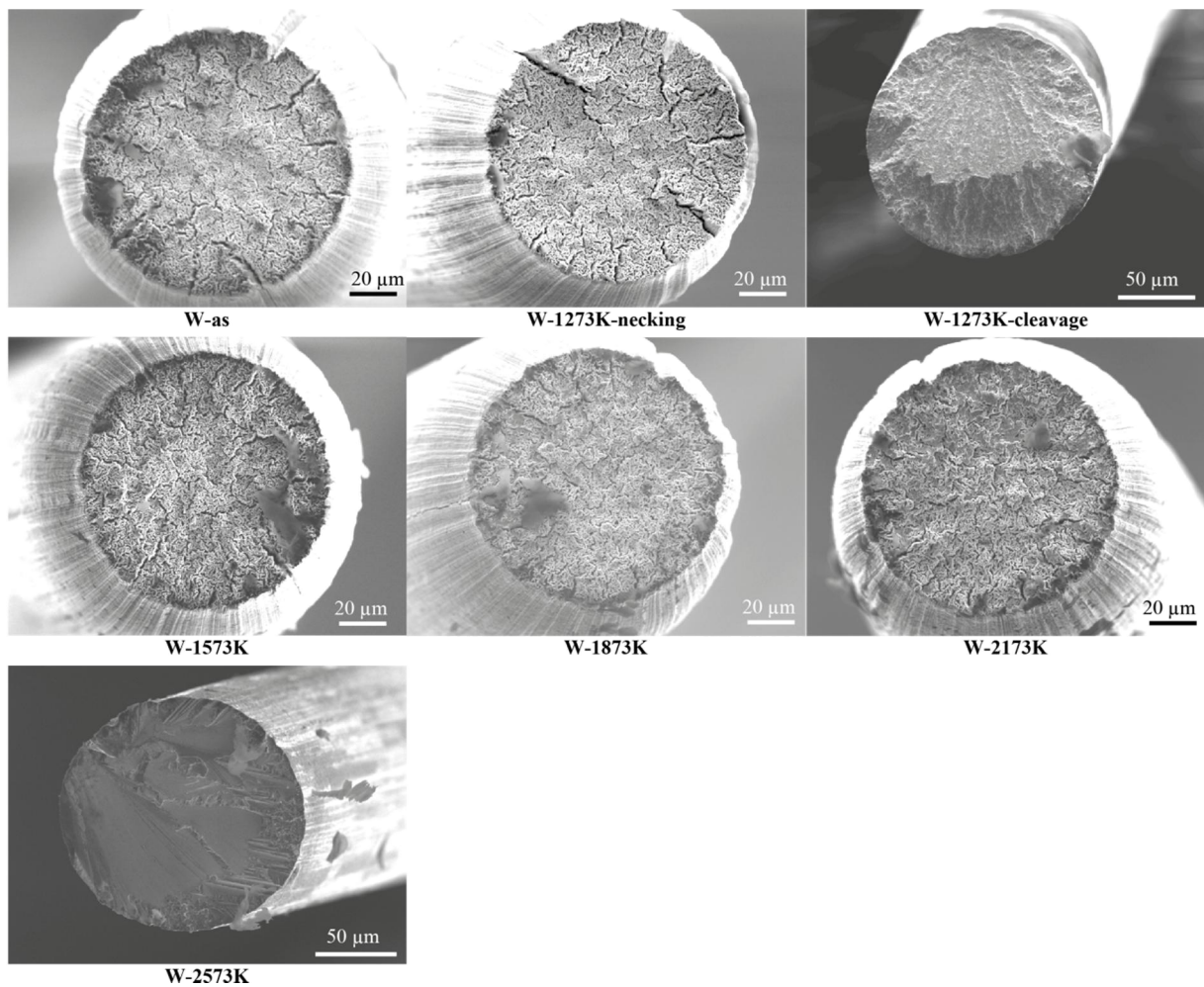
228 *Table 2: Ultimate strength of potassium doped tungsten wire with different annealing stages*  
 229 *determined in tensile tests.*

	<i>W-as</i>	<i>W-1273K</i>	<i>W-1573K</i>	<i>W-1873K</i>	<i>W-2173K</i>	<i>W-2573K</i>
<i>Ultimate Strength [MPa]</i>	2721±1	2409±6	2220±5	2089±4	1968±4	1274±26

230

231 Typical fracture surfaces for each sample type are shown in figure 6. Almost all fibres show  
 232 necking (reduction in cross-section) and a fibrous, knife edge necking dominated fracture  
 233 mode. Samples annealed at 1273 K without necking (missing step stress drop at the end of  
 234 tension test) and annealed at 2573 K show a cleavage dominated fracture.

235



236

237 *Figure 5: Typical fracture surfaces after tensile tests of potassium doped tungsten wire with*  
 238 *different annealing stages.*

239

240 **5. Discussion**

241 Most of the samples with an annealing temperature up to 2173 K show ductile behaviour with  
242 significant plastic deformation, a high fracture strain and pronounced necking. The fracture  
243 surfaces for these samples are typical for the ductile fracture of tungsten wire [22]. At first  
244 longitudinal grain boundaries debond leading to freestanding individual grains. Afterwards  
245 these grains neck down in a knife-edge fracture mode leading to a typical fibrous surface. For  
246 some samples annealed at 1273 K ductile behaviour without a dedicated necking regime is  
247 observed. These samples show a cleavage dominated fracture mode. All samples annealed at  
248 2573 K show pure elastic i.e. brittle behaviour with a cleavage dominated fracture mode.

249 To understand this behaviour the annealing behaviour and accordingly the recrystallization  
250 behaviour are important. Recrystallisation is difficult to tackle in doped tungsten wire as the  
251 processes are different compared to pure bulk tungsten [23]. Two distinct stages are  
252 identified: at first a relatively uniform coarsening sometimes referred to as primary  
253 recrystallization (starting at 1100 K) followed by a rapid growth of large elongated grains  
254 referred as secondary recrystallization or extensive grain growth (starting at 2200 K) [24].  
255 The first stage is assigned to polygonisation in which dislocations are organized into low  
256 angle boundaries [22] but also at this stage high angle boundary migration is active [25]. At  
257 the same time potassium bubble rows are formed at the grain boundaries inhibiting grain  
258 boundary migration in the radial direction. Thus the elongated grain structure is retained  
259 during grain coarsening until some grains reach the critical size (Hillerts criteria [26]) and  
260 show rapid grain growth. Also dragging of bubbles at this temperature can contribute to that  
261 effect [25].

262 As long as a relatively fine and elongated grain structure is preserved the amount of grain  
263 boundaries perpendicular to the tension load is small. Even if such boundaries debond they  
264 are bridged by adjacent long grains leading to a ductile behaviour. This seems to be the case  
265 until secondary grain growth occurs. The embrittlement is correlated with the occurrence of  
266 very large grains which facilitate cleavage.

267 In samples which were annealed at 1273 K, the reasons for the occurrence of cleavage and  
268 therefore the missing of necking are not obvious. For the occurrence of the knife edge fracture  
269 grain boundary debonding is necessary. The weakening of these boundaries by the formation  
270 of the potassium bubbles or by the interaction of longitudinal grain boundaries with these  
271 bubbles at increasing annealing temperature might be beneficial. In the as-fabricated stage the  
272 dislocations, which are present in a high amount, are able to move to the grain boundaries  
273 during loading and might have similar effects. The occurrence of cleavage at 1273 K  
274 annealing temperature is probably caused by a complicated interaction between annihilation  
275 of dislocations and formation of bubble rows and needs further investigation.

276 The as-fabricated wire shows a more pronounced strain hardening behaviour which can be  
277 attributed to the high density of dislocations due to the drawing process. With ongoing heat  
278 treatment the dislocation density decreases due to annihilation and grain coarsening.  
279 Therefore the blocking of dislocations is less pronounced and thus the work hardening rate is  
280 lower. For the same reason the yield strength decreases with rising annealing temperature.  
281 The strength stays around 2000 MPa until the very high annealing temperature where  
282 extensive grain growth and brittle behaviour occurs. All samples annealed at 1273 K show the  
283 same strength independent of the occurrence of necking. That means that there is no  
284 significant difference in the onset of ductile deformation. Leber et. al [22] also reported  
285 ductile deformation prior to cleavage fracture.

286  
287 The strength in the as-fabricated state is slightly smaller than reported previously for pure  
288 tungsten wire in similar tests [20]. The strength is influenced very much by the deformation  
289 rate and the annealing stages during fabrication [27] and was also reported to be higher in  
290 doped W wire in some cases [28]. Different fabrication histories are therefore most probably  
291 the cause for the differences in strength. The effect of decreasing work hardening capability  
292 with rising temperature is similar in both cases. The gain in fracture strain observed for doped

293 wires is not reported for pure W wire. This might be attributed to having fewer annealing  
294 stages but could also be caused by the faster loss of the elongated grain structure. The fracture  
295 modes are similar, knife necking of individual grains in the ductile case and cleavage  
296 dominated fracture in the brittle case. In pure W wire the embrittlement was correlated with  
297 the loss of elongated grain structure and not necessarily with the occurrence of  
298 recrystallization. Samples annealed at 1273K showed clear evidence of recrystallization but  
299 also clear ductile behaviour. This was attributed to the preserved elongated grain structure. In  
300 samples annealed at 1900 K this elongated structure was lost and the samples showed brittle  
301 behaviour. The elongated grain structure was therefore identified to be the key factor deciding  
302 whether there is ductile or brittle behaviour. In contrast to that the size of the grains plays an  
303 additional role in potassium doped wire. Very large grains provoke brittle fracture even  
304 though they are elongated. This size effect was probably not observed in pure W wire as here  
305 the grains lose their elongated shape much earlier due to the absences of the grain boundary  
306 pinning by potassium.

307 In summary similar effects seem to be valid in both pure and potassium doped tungsten wire.  
308 Annealing and even recrystallization leads at first to a decrease in work hardening capability  
309 most probably due to the decrease in dislocation density but not necessarily to embrittlement.  
310 Both types show ductile behaviour as long as an elongated fine grain structure is preserved.  
311 The main difference is that due to the potassium doping grain boundaries are pinned and this  
312 structure is preserved to much higher temperatures compared up to pure tungsten wire.

313

## 314 **6. Conclusion and outlook**

315 Tungsten fibre-reinforced composites feature unique properties which could allow their use in  
316 highly loaded areas of a future fusion reactor. However to reach this goal further development  
317 steps are necessary. The first step will be reached by producing mock-ups and testing them  
318 under cyclic high heat load. For this a multilayer approach is necessary addressing all

319 composite constituents and relevant manufacturing techniques. As an example the role of the  
320 tungsten wire used as fibre is discussed as for instance the properties of the wire are not only  
321 important for the composite properties but are also constraining the fabrication process.

322 Potassium doped tungsten wire was investigated by means of tensile tests in the as-fabricated  
323 and annealed states in order to investigate its use as fibre reinforcement in  $W_f/W$ . The main  
324 findings are:

- 325 • Potassium doped W wire annealed up to 2173 K shows ductile behaviour.
- 326 • Tensile strength stays about 2000 MPa up to annealing temperatures of 2173 K.
- 327 • Secondary grain growth at 2573 K leads to embrittlement

328 Similar to pure tungsten wire embrittlement is correlated with the loss of the fine elongated  
329 grain structure. To achieve a better understanding of the correlation between microstructure,  
330 i.a. dislocation density, grain size and aspect ratio, and mechanical behaviour a detailed  
331 EBSD study could be performed on the samples.

332 As potassium doped wire does not lose its good mechanical properties and in particular its  
333 ductile behaviour up to very high temperature the fabrication temperature of  $W_f/W$   
334 composites could be significantly increased. In addition the results are a strong indication that  
335 the application temperature of  $W_f/W$  might be increased if using doped wire. This has to be  
336 proven by investigating the mechanical properties of annealed  $W_f/W$  samples and by tensile  
337 tests of potassium doped W wire at an elevated temperature.

338

### 339 **Acknowledgements**

340 The authors want to acknowledge support by Osram GmbH, Schwabmünchen, Germany for  
341 providing the tungsten wire and M. Fuhr for his assistance in the metallographic preparations.

342 This work has been carried out within the framework of the EUROfusion Consortium and has  
343 received funding from the Euratom research and training programme 2014-2018 under grant

344 agreement No 633053. The views and opinions expressed herein do not necessarily reflect  
345 those of the European Commission.

346

## 347 **References**

- 348 [1] Coenen et al. Materials for DEMO and Reactor Applications - Boundary Conditions and New Concepts.  
349 *submitted to Physica Scripta (in this volume)*, PHYSSCR-103131, 2015
- 350 [2] N. Baluc. Final report on the EFDA task tw1-ttma-002 deliverable 5. *Technical report, Centre de*  
351 *Recherches en Physique de Plasmas*, 2002.
- 352 [3] R. Lässer, N. Baluc, J.-L. Boutard, E. Diegele, S. Dudarev, M. Gasparotto, A. Möslang, R. Pippan, B.  
353 Riccardi, and B. van der Schaaf. Structural materials for DEMO: The EU development, strategy, testing  
354 and modelling. *Fusion Engineering and Design*, **82**:511–520, 2007.
- 355 [4] J.-H. You and I. Komarova. Probabilistic failure analysis of a water-cooled tungsten divertor: Impact of  
356 embrittlement. *Journal of Nuclear Materials*, **375**:283–289, 2008.
- 357 [5] K.K. Chawla. Ceramic matrix composites. *Chapman & Hall*, 1993.
- 358 [6] J. Du. A Feasibility Study of Tungsten-Fiber-Reinforced Tungsten Composites with engineered  
359 interfaces. *Ph.D thesis, Technische Universität München*, 2011,  
360 <http://mediatum.ub.tum.de/node?id=998317>
- 361 [7] J. Riesch. Entwicklung und Charakterisierung eines wolframfaserverstärkten Wolfram-  
362 Verbundwerkstoffs. *Ph.D. thesis, Technische Universität München*, 2012,  
363 <http://mediatum.ub.tum.de/node?id=1106428>
- 364 [8] J. Du, T. Höschen, M. Rasinski, S. Wurster, W. Grosinger, and J.-H. You. Feasibility study of a tungsten  
365 wire reinforced tungsten matrix composite with ZrO<sub>x</sub> interfacial coatings. *Composites Science and*  
366 *Technology*, **70**:1483-1489, 2010.
- 367 [9] J. Du, T. Höschen, M. Rasinski, and J.-H. You. Interfacial fracture behavior of tungsten wire/tungsten  
368 matrix composites with copper-coated interfaces. *Materials Science and Engineering: A*, **527**:1623–  
369 1629, 2010.
- 370 [10] J. Riesch, J.-Y. Buffiere, T. Höschen, M. di Michiel, M. Scheel, Ch. Linsmeier, and J.-H. You. In-situ  
371 synchrotron tomography estimation of toughening effect by semi-ductile fibre reinforcement in a  
372 tungsten fibre-reinforced tungsten composite system. *Acta Materialia*, **61**:7060–7071, 2013.



- 373 [11] J. Riesch, J.-Y. Buffière, T. Höschen, M. Scheel, and J.-H. You. Crack bridging in as-produced and  
374 embrittled tungsten single fibre reinforced tungsten composites shown by a novel in-situ high energy  
375 synchrotron tomography bending test. *submitted to Acta Materialia*.
- 376 [12] J. Riesch, T. Höschen, Ch. Linsmeier, S. Wurster, and J-H You. Enhanced toughness and stable crack  
377 propagation in a novel tungsten fibre-reinforced tungsten composite produced by chemical vapour  
378 infiltration. *Physica Scripta*, **T159**:014031 (7pp), 2014.
- 379 [13] Materials Assessment Group. Assessment of the EU R&D Programme on DEMO Structural and High-  
380 Heat Flux Materials. Final report. 2012.
- 381 [14] Mankins, J.C.. Technology readiness assessments: A retrospective. *Acta Astronautica*, **65**:1216-  
382 1223,2009.
- 383 [15] D. Stork. Developing Structural, High-heat flux and Plasma Facing Materials for a near-term DEMO  
384 Fusion Power Plant: the EU Assessment. *16<sup>th</sup> International Conference on Fusion Reactor Materials*,  
385 Beijing, 2013.
- 386 [16] H. Greuner et al. Design, performance and construction of a 2MW ion beam test facility for plasma  
387 facing components. *Fusion Engineering and Design*, **75–79**:345–350, 2005.
- 388 [17] H. Greuner, B. Böswirth, J. Boscary und P. McNeely. High heat flux facility GLADIS: Operational  
389 characteristics and results of W7-X pre-series target tests. *Journal of Nuclear Materials*, **367–370**:1444–  
390 1448, 2007.
- 391 [18] R. Duwe, W. Kühnlein, and H. Münstermann. The new Electron Beam Facility for Materials Testing in  
392 Hot Cells. *Fusion Technology*, 356-358, 1995.
- 393 [19] B. Jasper, J.W. Coenen, J. Riesch, T. Höschen, M. Bram, and Ch. Linsmeier. Powder Metallurgical  
394 Tungsten Fiber-Reinforced Tungsten. *Materials Science Forum*, Vols **825-826**:125-133, 2015.
- 395 [20] P. Zhao, J. Riesch, T. Höschen, J. Almanstötter M. Balden, J.W. Coenen, and R. Neu. Microstructure,  
396 mechanical behavior and fracture of pure tungsten wires after different heat treatments. *submitted to*  
397 *International Journal of plasticity*.
- 398 [21] C.L. Briant, O. Horacek, and K. Horacek. The Effect of Wire History on the Coarsened Substructure  
399 and Secondary Recrystallization of Doped Tungsten. *Metallurgical Transactions A*. 24A:849-851 ,  
400 1993.
- 401 [22] S. Leber, J. Tavernelli, and D.D. White. Fracture modes in tungsten wire. *Journal of the Less-Common*  
402 *Metals*, **48**:119-133, 1976.

- 403 [23] L. Uray, A. Sulyok, and P. Tekula-Buxbaum. Factors Influencing the Recrystallization of Non-Sag  
404 Tungsten Wires Indicated by the Out-Diffusion of Cobalt. *High Temperature Materials and Processes*,  
405 **24-5**:289-299, 2005.
- 406 [24] D.B. Snow. The recrystallization of non-sag tungsten wire. In The metallurgy of doped/non-sag  
407 tungsten. *Elsevier Applied Science*, 1989
- 408 [25] D.B. Snow. The Recrystallization of Heavily-Drawn Doped Tungsten Wire. *Metallurgical Transactions*  
409 *A*. 7A:783-794 , 1976.
- 410 [26] M. Hillert. On the theory of normal and abnormal grain growth. *Acta Metallurgica*, 13:227-238, 1965.
- 411 [27] J.A. Mullendore. The technology of doped-tungsten wire manufacturing. In The metallurgy of  
412 doped/non-sag tungsten. *Elsevier Applied Science*, 1989
- 413 [28] E. Pink, and I. Gaal. Mechanical properties and deformation mechanism of non-sag tungsten wires. In  
414 The metallurgy of doped/non-sag tungsten. *Elsevier Applied Science*, 1989